Self-Assembly

DOI: 10.1002/anie.201

An Exceptionally Stable and Scalable Sugar-Polyolefin Frank-Kasper A15 Phase

*Kätchen K. Lachmayr, Charlotte M. Wentz, and Lawrence R. Sita**

Periodically-ordered, 'one-component' soft material Frank-Kasper (FK) phases, which arise from the topological close packing (TCP) of 'deformable' sphere-shaped particles, have now been experimentally verified for amphiphilic liquid crystals and dendrons, block copolymers, 'giant' molecules and surfactants, and colloidal nanoparticles.[1-9] Frank and Kasper[10] originally developed the concept of TCP to rationalize how the complex crystal structures of certain intermetallic alloys arise through the packing of asymmetric polyhedral that are associated with different sets of atoms that define a particular coordination number, CNx, where x = 12, 14, 15, or 16. For example, as shown in Fig. 1, the unit cell of the cubic FK A15 ($Pm\bar{3}n$) phase, which is found for some bimetallic alloys with A_3B stoichiometry (e.g. Nb_3Sn), can be seen as arising from two crystallographically equivalent B sites that reside within CN12 distorted icosahedra, while six equivalent face-shared A sites are associated with CN14 polyhedra. Other commonly encountered bimetallic FK phases include the Laves C14 and C15 structures for A_2B alloys (e.g. $MgZn_2$), and the complex σ phase for AB alloys of indeterminate stoichiometry (e.g. CrFe) that is comprised of atoms that are now grouped into five different sets within a tetragonal unit cell. The FK σ phase can also be viewed as an approximate for a non-periodic dodecagonal quasicrystal (DQC) structure.[11,12] Given the successful material science of 'hard' sphere FK phases, which includes the discovery of superconducting properties for A15 bimetallics[13], one of the primary interests in the occurrence of similar one-component soft matter FK phases is the desire to understand the underlying principles and mechanisms by which an initial set of identical spherical particles can be driven to reconfigure and self-sort into two or more sets with different size or shape, and importantly, with different free energies.[14,15] Unfortunately, based on the structures and properties of the extremely small number of soft matter FK phases reported to date, significant barriers to answering this question, and others, currently exist, and these include, undefined or limiting mechanisms and processes for thermotropic self-assembly, low thermodynamic or kinetic stability, and low-yielding syntheses of structurally-complex precursor materials. For the discovery of new physical properties and phenomena, and ultimately, new technological innovations that are beneficial to society, it is also attractive, or perhaps even critical, if the scalable production of practical quantities of new soft matter FK phases can be achieved within the range of a few grams to up to several kilotons using short and reproducible synthetic schemes that are based on inexpensive, readily-available, and sustainable feedstocks. Herein, we report the serendipitous discovery that the one-component sugar-polyolefin conjugate derivative represented by triazole-linked, cellobiose-*atactic* poly(4-methyl-1-pentene) (CB-aPMP) **1** of Fig. 2 is capable of forming a soft matter FK A15 phase through a self-assembly process that proceeds through fast and *irreversible* thermotropic order-order transitions involving an initial hexagonal cylindrical (*C*)

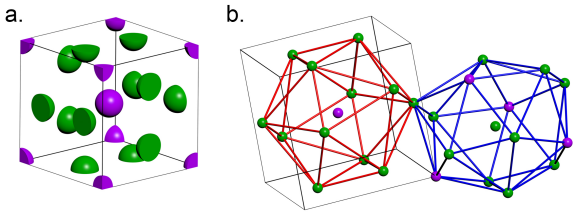

Fig. 1. Representations of the cubic Frank-Kasper A15 phase with space group $Pm\bar{3}n$ showing (a) the unit cell content for a typical A_3B bimetallic alloy with two crystallographically-equivalent corner and center B atoms (purple) and six equivalent face-shared A atoms (green), and (b) distorted polyhedral centered on B atoms with CN12 (red) and on A atoms with CN14 (blue). Note that B and A atoms in (a) and (b) are represented by spheres of arbitrary but equal size.

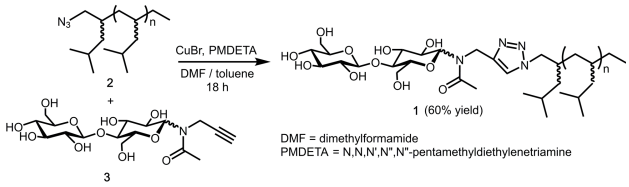

Fig. 2. Structure and synthesis of sugar-polyolefin conjugate **1**.

phase and a transient A15 intermediate. Importantly, upon cooling to room temperature, this final A15 phase of **1** displays exceptional stability in the solid state by remaining unchanged after storage under ambient conditions for, at least, three months, and after repetitive thermal cycling between 25 °C and 180 °C. A proposed new, and potentially general, mechanism that accounts for these observations is based on a symmetry-allowed epitaxial transition pathway that uniquely avoids the need to invoke either dynamic mass transfer of molecular components between spheres or large structural reorganizations in the bulk to occur in order to establish unit cell non-equivalency of particles. Since a wide variety of sugar-polyolefin conjugates, including **1**, can indeed be obtained through simple synthetic routes in practical quantities from readily-available and sustainable precursors, our results serve to establish a potential path to viable scalable production and technological innovations of stable sugar-polyolefin FK A15 phases that further have the benefit of possessing intrinsic chirality and chemical reactivity that are associated with the sugar domain.

We have previously reported that sugar-polyolefin conjugates can be conveniently obtained through the chemical linking of a polar saccharide 'head' group with a hydrophobic 'tail' derived from an end-group functionalized poly(α-olefinate) (xPAO) of tunable molecular weight and very narrow molecular weight distribution, also known as polydispersity.[16,17] The xPAO precursors are, in turn, prepared through the transition-metal-mediated living coordinative chain transfer polymerization (LCCTP) of a common α-olefin monomer, such as propene and 4-methyl-1-pentene (4M1P).[18] Importantly, through programmed variations in molecular weight and the space-filling requirements of the polyolefin pendant side chain, a

[*] K. K. Lachmayr, C. M. Wentz and Prof. L. R. Sita
Department of Chemistry and Biochemistry
University of Maryland, College Park, MD 20742 (USA)
E-mail: lsita@umd.edu

Supporting information for this article is available on the WWW under http://dx.doi.org/10.1002/anie.201xxxxxx.

wide variety of occupied free volumes for the hydrophobic domain of sugar-polyolefin conjugates can be easily designed and synthesized.[16]

In the present report, ultra-low molecular weight amorphous, *atactic* azido-terminated poly(4-methyl-1-pentene) (N_3-aPMP) (**2**), with a number-average molecular weight index, M_n, of 1.0 kDa and a polydispersity index, $Đ$ (= M_w/M_n), of 1.05, where M_w is the weight-average molecular weight index, was prepared through the LCCTP of a fixed amount of 4M1P using previously published methods.[16,18] As shown in Fig. 2, sugar-polyolefin conjugate **1** was next prepared in high yield through the copper-mediated 'click' reaction between **2** and the cellobiose propargyl amide derivative **3**. After purification, matrix-assisted laser desorption ionization (MALDI) mass spectrometry of **1** provided M_n and $Đ$ values of 1.4 Da and 1.05, respectively, and this material was shown to exist by ^{1}H NMR spectroscopy as a non-interconverting 3 : 1 mixture of β and α stereochemical anomers.

Thermal analysis of **1** conducted using differential scanning calorimetry (DSC) between -70 °C to 200 °C revealed glass transition temperatures, T_g, of 19 °C and 80 °C that are assigned to the aPMP and CB domains, respectively. However, given the hybrid nature of the sugar-polyolefin structure, we view **1** as neither bearing the traits of a conventional liquid crystal nor of a block copolymer. Thermal stability of **1** was further assessed by a thermogravimetric analysis (TGA) conducted under an inert atmosphere of dinitrogen, and this study showed that significant weight loss only starts to occur above 250 °C, which we assign as the lowest decomposition temperature limit. Notably, the lack of any appreciable weight loss below this temperature is taken to signify that **1** is not hygroscopic, nor does it retain water or other polar impurities in the solid state. Finally, we have previously documented that sugar-polyolefin conjugates that incorporate a low molecular weight, amorphous *atactic* polypropene domain undergo microphase separation within ultrathin films as evidenced by surface structural analysis using phase-sensitive, tapping mode atomic force microscopy (ps-tm AFM).[16,17] However, similar ps-tm AFM characterization of unannealed and thermally-annealed (e.g., 130 °C for 18 h) ultrathin films of **1** supported on both hydrophobic and hydrophilic substrates revealed only featureless surfaces.

In contrast to the less-than-promising AFM results for **1**, a preliminary routine variable-temperature synchrotron small angle x-ray scattering (SAXS) investigation performed with a bulk sample uncovered surprising evidence for a rich thermotropic phase behavior. Fig. 3 presents selected 1D SAXS results that were collected at intervals of time and temperature during a heating temperature ramp profile of 1 °C / min performed over the range of 30 °C to 220 °C with a 10 second exposure time for each data set. Between data collections, the sample holder was incrementally rastered to a new position in order to minimize beam damage. Finally, the upper temperature of 220 °C was selected to be well below the onset of thermal decomposition. However, even then, it must be noted that solid samples of **1** were always observed to visually darken upon heating *in vacuo* to this temperature

As shown in Fig. 3a, a nascent hexagonal phase of **1** was first observed to exist at 31 °C for a bulk sample that had no prior thermal history. Between this temperature and 136 °C, clear evidence for formation of a highly ordered hexagonal cylindrical (*C*) morphology was now obtained with q/q* peaks appearing at 1, $\sqrt{3}$, $\sqrt{4}$, $\sqrt{7}$, and $\sqrt{9}$ (q* =0.1294 Å^{-1}) for the 136 °C data set that are indexed to the *hkl* Miller planes of (100), (110), (200), (210), and (300), respectively (see Fig. 3b). Upon increasing temperature further, *C* continued to be the only phase for **1** that was present up to a temperature of 145 °C, at which point, a new phase for **1** started to appear and continue to grow in at the expense of *C* through an apparent order-order phase transition (*cf,* SAXS results for 157 °C and 181 °C of Fig. 3a). Quite surprisingly, however, above 181 °C, this new second phase of **1** was shown to be only transient in nature, and it too appeared to convert to a final third phase through another order-order transition until the latter was the only phase observed at 212 °C and up to the temperature

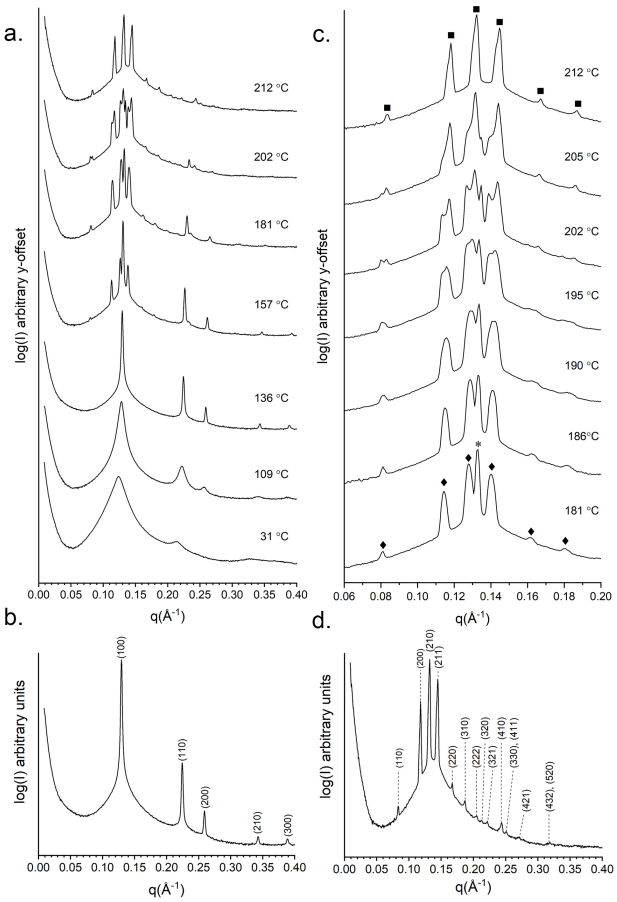

Fig. 3. (a) Selected synchrotron 1D SAXS data for a solid sample of **1** obtained at fixed time intervals during a heating rate of 1 °C / min starting from an initial temperature of 30 °C and up to a final temperature of 220 °C. (b) SAXS data from (a) at 136 °C with *hkl* Miller indices assigned for a hexagonal cylindrical (*C*) phase. (c) Additional selected SAXS data obtained in (a) with expanded x-axis showing coexistence of *C* (*), a transient FK A15$_t$ phase (♦) and a final equilibrium FK A15$_e$ (■). (d) SAXS data from (a) at 212 °C with *hkl* Miller indices assigned for the FK A15$_e$ phase.

limit of 220 °C. As highlighted with additional selective SAXS data from this same temperature ramp experiment that are reproduced in Fig. 3c, it is interesting to note that within the temperature range of 195 °C to 205 °C, all three phases of **1** were seen to coexist, which is a highly rare phenomenon for the thermotropic phase behavior of soft materials.[19] Finally, the number and pattern of intensities for the scattering peaks observed in the 1D SAXS data for both of the two new phases of **1** are signatures for the cubic FK A15 unit cell structure.[1-9] Indeed, thirteen peaks at q/q* = $\sqrt{2}, \sqrt{4}, \sqrt{5}, \sqrt{6}, \sqrt{8}, \sqrt{10}, \sqrt{12}, \sqrt{13}, \sqrt{14}, \sqrt{17}, \sqrt{18}, \sqrt{21}, \sqrt{29}$ were successfully matched to those expected for this particular FK phase at 195 °C, with q* = 0.0805 Å^{-1} for the 'transient' phase, A15$_t$, and q* = 0.0823 Å^{-1} for the final equilibrium structure, A15$_e$ (see Fig. 3c). In further support of this structural assignment, Fig 3d provides the corresponding assignments of the *hkl* Miller planes to the scattering peaks observed for the pure A15$_e$ phase obtained at 212 °C.

Structural parameters for the *C*, A15$_t$ and A15$_e$ phases of **1** were derived from the variable temperature SAXS data of Fig 3 in standard fashion. Of particular interest is the observation that the cylinder-to-cylinder domain spacing for *C*, $d_c = 2(d_{110})$, where $d_{110} = 2\pi/(q_{110})$, is observed to decrease in a linear fashion as temperature is increased, and more specifically, with a 4.1% decrease starting from an initial d_c value of 5.84 nm at 31 °C to only 5.61 nm at 136 °C. This trend in decreasing d_c value continues at temperatures where coexistence with the two A15 phases occurs, however, it is possible that more than one dynamic process may be responsible within this temperature range (*vide infra*). Finally, for the two cubic FK phases, A15$_t$ and A15$_e$, the

SAXS data analysis provided relatively close values for the unit cell length, a, for temperatures at which the two phases coexist, and more specifically, a_t = 11.10 nm and a_e = 10.81 nm, respectively at 195 °C. However, a significantly larger difference was observed at 212 °C, with the latter now having a calculated a_e value of only 10.58 nm, which represents a 4.7% decrease relative to the former. Regarding long-term stability, an isothermal experiment was conducted using an in-house SAXS instrument at a fixed temperature of 180 °C and over a time period of 900 min. Importantly, as the data provided in the Supporting Information confirm, *C* cleanly converted once again to the final $A15_e$ phase, but in this study, no evidence for the $A15_t$ intermediate phase was now seen, potentially due to the equilibrating conditions of this study. As noted previously, an additional surprising finding was that a pure $A15_e$ phase obtained by thermal annealing of **1** at 180 °C remained unchanged after being cooled to room temperature, and this stability was seen to persist for extended periods of time under ambient conditions and upon repeated thermal cycling. To the best of our knowledge, the thermodynamic and kinetic stability of the $A15_e$ phase of **1** is unprecedented vis-à-vis all other reports of soft matter A15 phases obtained through a phase transition.

To obtain more structural information, a le Bail refinement of the synchrotron SAXS data for the $A15_e$ phase of **1** obtained at 212 °C was performed using the JANA2006 program to provide a calculated set of *hkl* reflections and intensities that were then used as input for a SUPERFLIP computational reconstruction of the three-dimensional electron density for this structure which is displayed in Fig. 4.[20,21] In keeping with similar analyses performed for other soft matter FK A15 phases, we interpret the high electron density regions shown in the unit cell of Fig 4a as being associated with the sugar domains of core-shell micelles formed from **1** while the colorless region is occupied by aPMP hydrocarbon chains. For the corner and center 'B sites' (*cf.* Fig 1a), these micelle cores adopt a near-spherical geometry, whereas in the 'A sites', the sugar domains are now more decidedly oblate in shape. Finally, while the A15 structure is reproduced each time, separate solutions provided by SUPERFLIP have yielded relative volumes that range from the A site being 0 to 25% larger than the B site and this variance is likely due to the quality of the experimental SAXS data and refinement that has been acquired to date. With respect to the extended structure, Fig. 4b and Fig. 4c provide different perspectives of the electron density map for a 4x2 lattice of eight unit cells in which three orthogonally-aligned chains of A sites can now be seen as one of the well-recognized features of the A15 phase. We also present a unique perspective that is presented in Fig. 4d of the electron density for this 4x2 lattice that is now oriented normal to one set of the 3-fold proper rotation axes that are centered along chains of B sites. Most notably, this last perspective serves to highlight the existence of 3_1 screw axes defined by helical chains of A sites that are arranged in alternating clockwise and counter-clockwise fashion about each of the 3-fold proper rotation axes. We believe that recognition of this last set of symmetry elements is key to understanding the mechanism for highly efficient thermotropic self-assembly of **1** into an exceptionally stable FK A15 phase.

To begin, low-level molecular mechanic simulations show that the aPMP fragment of **1** can adopt both wedge- and cone-shaped space-filling conformations, with the latter being favored at higher temperatures. In this manner, aPMP fulfills the role previously played by the highly branched dendrons of a dendritic liquid crystal that initially forms a hexagonal columnar *C* phase through the self-assembly of wedge-shaped molecular units.[22] Upon heating, however these dendrons convert to cone-shaped units that drive the conversion of cylinder domains into a hexagonal array of stacked spherical particles that then undergo rearrangement to provide an A15 structure.[2] Although this *reversible* thermotropic $C \leftrightarrow$ A15 transition has been proposed to proceed in epitaxial fashion, specific mechanistic details are lacking other than to recognize that large structural reorganization of spherical particles within the bulk is not likely to be occurring.[23] Similar transformations of cylinders into stacks of spherical particles have been proposed for block copolymers

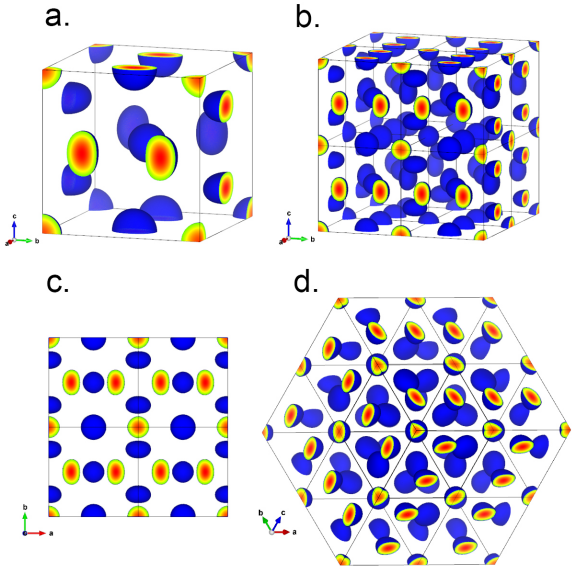

Fig. 4. Experimentally derived electron density maps for the FK $A15_e$ phase of **1** and displayed as (a) a single unit cell and (b-d) for different orientations of a 4x2 lattice of eight unit cells.

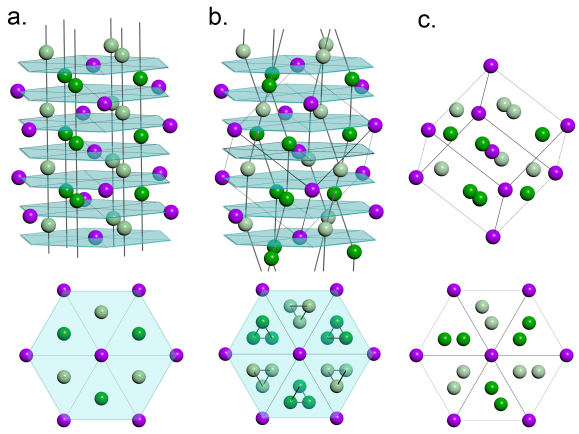

Fig. 5. Proposed mechanism for solid-state epitaxial order-order transition between rhombohedral to cubic A15 phases via structural displacements of linear chains of spherical particles shown in the oblique (upper) and top (lower) views of (a) to form alternating 3_1 (light green) and 3_2 (dark green) helical chains in the corresponding oblique and top views of (b). In (c), removal of all features lying outside the boundaries of a cube with sides of length, a_{A15}, serves to generate the unit cell of the A15 phase.

undergoing an order-order transition between *C* and body-centered cubic (BCC) phases.[19,24,25] Accordingly, it is reasonable to assume a similar first step in the $C \rightarrow$ A15 transition pathway for **1**, which is further supported by the significant reduction in inter-cylinder spacing that is observed as these domains are presumed to narrow in diameter and elongate prior to 'pinching off' to form stacks of spheres. Next, since a direct transition between hexagonal and cubic structures is not formally allowed on the basis of symmetry restrictions, small inter- and intra-layer displacements can convert an initial hexagonal co-facial layered AAA stacking of spheres into a rhombohedral ABC stacking arrangement. Indeed, similar hexagonal to rhombohedral structural transitions have been reported for stacked columns of spherical Au nanoparticles that also form ABC layered structures similar to that depicted at left in Fig. 5.[26,27] Finally, since rhombohedral to cubic transitions are also symmetry-allowed, and as Fig. 5 further reveals, we propose that in the present case, this occurs through a simple structural displacement of linear chains of spheres

into alternating 3_1 helical arrangements according to Fig. 5a and 5b. As can be seen in the top views of these figures, a driving force for this linear to helical chain structural change could be to maximize packing of spheres within the triangular interstitial spaces of the hexagonal layer. Further, since any movement along this transition pathway is sufficient to generate an A15 structure (see Fig. 5c) this proposed mechanism provides support for initial formation of a transient A15 intermediate that then transitions to a final equilibrium A15 phase through a unit cell contraction that might occur with subsequent deformation of the spherical shape of particles at A sites. A similar occurrence of a transient BCC phase has been reported for a $C \rightarrow$ BCC order-order transition of a diblock copolymer.[25] Finally, we speculate that the significant amount of lattice parameter contraction that occurs in the $C \rightarrow A15_t \rightarrow A15_e$ transition path provides a high energy barrier for the reverse process, and accordingly, a high degree of kinetic stability for the final $A15_e$ phase of **1**.

A unique feature of the $C \rightarrow$ A15 transition mechanism proposed in Fig. 5 is that it avoids the need to invoke any large structural reorganizations of spheres, such as spatial translocation between different cylindrical columns[9a], as well as, dynamic mass transfer of components between spheres to establish sets with different sizes that then go on to form various FK phases. This latter mass-transfer mechanism has been championed as a way to rationalize the emergence of a variety of FK phases of block copolymers from the melt or disordered state, and it has received strong support from computational models based on self-consistent field theory.[4c,14,15,28-30] Although we do not dispute that this bulk mass transfer mechanism might be operative for block copolymers under the conditions reported, we also strongly believe that further development of the area of soft matter FK phases will be severely limited if the mass-transfer process represents the only way to access these novel structural forms. In this regard, although the mechanism of Fig. 5 might also be limited to the facile formation of only A15 phases, it nonetheless provides a realistic strategy for designing and targeting derivatives with much higher molecular weights that can potentially provide access to significantly larger A15 unit cells that are required for some potential applications, such as photonic crystals. Here, it is notable that a wide variety of soft materials are well known to assemble into the commonly encountered *C* morphology. As a final point, we believe that the ease of scalable production of a wide spectrum of different derivatives of sugar-polyolefin conjugates can significantly lower the barrier to the future scientific and technological development of one-component soft matter FK phases.

Acknowledgements

This research used resources of the Center for Functional Nanomaterials and the National Synchrotron Light Source II, which are U.S. DOE Office of Science Facilities, at Brookhaven National Laboratory under Contract No. DE-SC0012704. We thank the National Science Foundation for support for the acquisition of SAXS and AFM instruments (DMR-1228957 and MRI 1626288, respectively) and high field 800 MHz and solid state 500 MHz NMR spectrometers (BDI-1040158 and MRI 1726058, respectively).

Experimental Section

Complete experimental details are provided in the Supporting Information.

Received: ((will be filled in by the editorial staff))
Published online on ((will be filled in by the editorial staff))

Keywords: thermotropic • self-assembly • polyolefin • Frank-Kasper

[1] (a) K. Borisch, S. Diele, P. Göring, C. Tschierske, *Chem. Commun*. **1996**, 237-238. (b) K. Borisch, S. Diele, P. Göring, H. Kresse, C. Tschierske, *Angew. Chem. Int. Ed. Engl*. **1997**, *36*, 2087-2089. (c) K. Borisch, S. Diele, P. Göring, H. Müller, C. Tschierske, *Liq. Crys*. **1997**, *22*, 427-443. (d) K. Borisch, S. Diele, P. Göring, H. Kresse, C. Tschierske, *J. Mater. Chem*. **1998**, *8*, 529-543. (e) H. Dai, X. Yang, X. Tan, F. Su, X. Cheng, F. Liu, C. Tschierske, *Chem. Commun*. **2013**, *49*, 10617-10619.

[2] (a) V. S. K Balagurusamy, G. Ungar, V. Percec, G. Johansson, *J. Am. Chem. Soc.* **1997**, *119*, 1539-1555. (b) S. D. Hudson, H.-T. Jung, V. Percec, W.-D. Cho, G. Johansson, G. Ungar, V. S. K. Balagurusamy, *Science* **1997**, *278*, 449-452. (c) V. Percec, C.-H. Ahn, G. Ungar, D. J. P. Yeardley, M. Möller, S. S. Sheiko, *Nature* **1998**, *391*, 161-164. (d) G. Ungar, Y. Liu, X. Zeng, V. Percec, W.-D. Cho, *Science* **2003**, *299*, 1208-1211. (e) V. Percec, M. R. Imam, M. Peterca, D. A. Wilson, R. Graf, H. W. Spiess, V. S. K. Balagurusamy, P. A. Heiney, *J. Am. Chem. Soc*. **2009**, *131*, 7662-7677. (f) B M. Rosen, D. A. Wilson, C. J. Wilson, M. Peterca, B. C. Won, C. Huang, L. R. Lipski, X. Zeng, G. Ungar, P. A. Heiney, V. Percec, *J. Am. Chem. Soc.* **2009**, *131*, 17500-17521. (g) M. N. Holerca, D. Sahoo, B. E. Partridge, M. Peterca, X. Zeng, G. Ungar, V. Percec, *J. Am. Chem. Soc.* **2018**, *140*, 16941-16947. (h) D. A. Wilson, K. A. Andreopoulov, M. Peterca, P. Leowanawat, D. Sahoo, B. E. Partridge, Q. Xiao, N. Huang, P. A. Heiney, V. Percec, *J. Am. Chem. Soc*. **2019**, *141*, 6162-6166.

[3] B.-K. Cho, A. Jain, S. M. Gruner, U. Wiesner, *Science* **2004**, *305*, 1598-1601.

[4] (a) S. Lee, M. J. Bluemle, F. S. Bates, *Science* **2010**, *330*, 349-353. (b) S. Chanpuriya, K. Kim, J. Zhang, S. Lee, A. Arora, K. D. Dorfman, K. T. Delaney, G. H. Fredrickson, F. S. Bates, *ACS Nano* **2016**, *10*, 4961-4972. (c) K. Kim, M. W. Schulze, A. Arora, R. M. Lewis, III, M. A. Hillmyer, K. D. Dorfman, F. S. Bates, *Science* **2017**, *356*, 520-523.

[5] M. W. Bates, J. Lequieu, S. M. Barbon, R. M. Lewis III, K. T. Delaney, A. Anastasaki, C. J. Hawker, G. H. Fredrickson, C. M. Bates, C. M. *Proc. Natl. Acad. Sci. USA* **2019**, *116*, 13194-13199.

[6] (a) M. Huang, C.-H. Hsu, J. Wang, S. Mei, X. Dong, Y. Li, M. Li, H. Liu, W. Zhang, T. Aida, W.-B. Zhang, K. Yue, S. Z. D. Cheng, *Science* **2015**, *348*, 424-428. (b) K. Yue, M. Huang, R. L. Marson, J. He, J. Huang, Z. Zhou, J. Wang, C. Liu, X. S. Yan, K. Wu, Z. Guo, H. Liu, W. Zhang, P. Ni, C. Wesdemiotis, W.-B. Zhang, S. C. Glotzer, S. Z. D. Cheng, *Proc. Natl. Acad. Sci. USA* **2016**, *113*, 14195-14200. (c) Z. Su, C.-H. Hsu, Z. Gong, X. Feng, J. Huang, R. Zhang, Y. Wang, J. Mao, C. Wesdemiotis, T. Li, S. Seifert, W. Zhang, T. Aida, M. Huang, S. Z. D. Cheng, *Nature Chem*. **2019**, *11*, 899-905.

[7] S. Hajiw, B. Pansu, J.-F. Sadoc, *ACS Nano* **2015**, *9*, 8116-8121.

[8] M. Girard, S. Wang, J. S. Du, A. Das, Z. Huang, V. P. Dravid, B. Lee, C. A. Mirkin, M. O. de la Cruz, *Science* **2019**, *364*, 1174-1178.

[9] FK phases have also been established for 'two-component' systems consisting of lyotropic (solvent) mesophases of an amphiphile or those derived from the thermotropic self-assembly of blends of amphiphiles, see, for instance: (a) P. Mariani, L. Q. Amaral, L. Saturni, H. Delacroix, *J. Phys. II France* **1994**, *4*, 1393-1416. (b) D. V. Perroni, M. K. Mahanthappa, *Soft Matter* **2013**, *9*, 7919-7922. (c) S. A. Kim, K.-J. Jeong, A. Yethiraj, M. K. Mahanthappa, *Proc. Natl. Acad. Sci. USA* **2017**, *114*, 4072-4077. (d) A. Jayaraman, D. Y. Zhang, B. L. Dewing, M. K. Mahanthappa, *ACS Cent. Sci.* **2019**, *5*, 619-628. (e) K. Borisch, C. Tschierske, P. Göring, S. Diele, *Chem. Commun*. **1998**, 2711-2712. (f) H. Y. Jung, M. J. Park, Soft Matter **2016**, *13*, 250-257.

[10] (a) F. C. Frank, J. S. Kasper, *Acta Crystallogr.* **1958**, *11*, 184-190. (b) F. C. Frank, J. S. Kasper, *Acta Crystallogr.* **1959**, *12*, 483-499.

[11] X. Zeng, G. Ungar, Y. Liu, V. Percec, A. E. Dulcey, J. K. Hobbs, *Nature* **2004**, *428*, 157-160.

[12] T. M. Gillard, S. Lee, F. S. Bates, *Proc. Natl. Acad. Sci., USA* **2016**, *113*, 5167-5172.

[13] G. R. Stewart, *Physica C: Superconductivity and Its Applications*, **2015**, *514*, 28-35.

[14] S. Lee, C. Leighton, F. S. Bates, *Proc. Natl. Acad. Sci. USA* **2014**, *111*, 17723-17731.

[15] A. Reddy, M. B. Buckley, A. Arora, F. S. Bates, K. D. Dorfman, G. M. Grason, *Proc. Natl. Acad. Sci. USA* **2018**, *115*, 10233-10238.

[16] T. S. Thomas, W. Hwang, L. R. Sita, *Angew. Chem. Int. Ed.* **2016**, *55*, 4683-4687.

[17] S. R. Nowak, W. Hwang, L. R. Sita, *J. Am. Chem. Soc.* **2017**, *139*, 5281-5284.
[18] W. Zhang, L. R. Sita, *J. Am. Chem. Soc*. **2008**, *130*, 442-443.
[19] M. J. Park, J. Bang, T. Harada, K. Char, T. P. Lodge, *Macromolecules* **2004**, *37*, 9064-9075.
[20] V. Pet říček, M. Dušek, L. Palatinus, *Z. Kristallogr.* **2014**, *229*, 345-352.
[21] L. Palantinus, G. Chapuis, *J. Appl. Cryst*. **40**, 786-790.
[22] H.-J. Sun, S. Zhang, V. Percec, *Chem. Soc. Rev*. **2015**, *44*, 3900-3923.
[23] M. Peterca, M. R. Imam, S. D. Hudson, B. E. Partridge, D. Sahoo, P. A. Heiney, M. L, Klein, V. Percec, *ACS Nano* **2016**, *10*, 10480-10488.
[24] C. Y. Ryu, T. P. Lodge, *Macromolecules* **1999**, *32*, 7190-7201.
[25] K, Kimishima, K. Saijo, T. Koga, T. Hashimoto, *Macromolecules* **2013**, *46*, 9032-9044.
[26] X. Zeng, F. Liu, A. G. Fowler, G. Ungar, L. Cseh, G. H. Mehl, J. E. Macdonald, *Adv. Mater*. **2009**, *21*, 1746-1750.
[27] K, Kanie, M. Matsubara, X. Zeng, F. Liu, G. Ungar, H. Nakamura, A. Muramatsu, *J. Am. Chem. Soc.* **2012**, *134*, 808-811.
[28] R. M. Lewis, III, A. Arora, H. K. Beech, B. Lee, A. P. Lindsay, T. P. Lodge, K. D. Dorfman, F. S. Bates, *Phys. Rev. Lett.* **2018**, *121*, 208002(1-5).
[29] A. Arora, J. Qin, D. C. Morse, K. T. Delaney, G. H. Fredrickson, F. S. Bates, K. D. Dorfman, *Macromolecules* **2016**, *49*, 4675-4690.
[30] W. Li, C. Duan, A.-C. Shi, *ACS Macro Lett*. **2017**, *6*, 1257-1262.

Self-Assembly

Kätchen K. Lachmayr, Charlotte M. Wentz and Lawrence R. Sita* **Page – Page**

An Exceptionally Stable and Scalable Sugar-Polyolefin Frank-Kasper A15 Phase

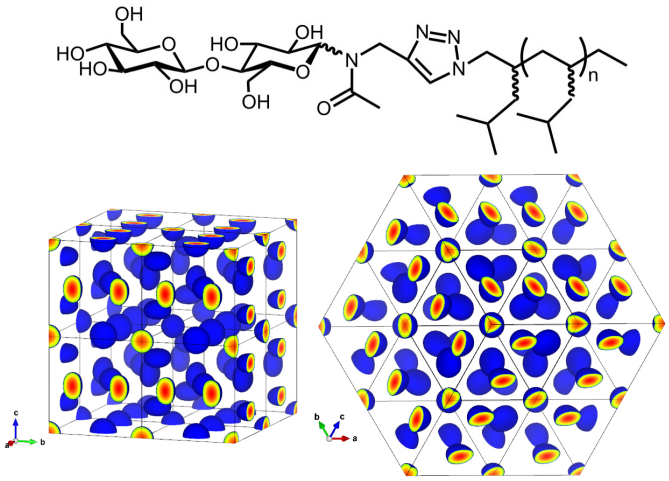

Solid-state 'one-component' soft material Frank-Kasper (FK) phases are a new structural form of matter that possess periodically ordered structures arising from the self-reconfiguration and close packing of an initial assembly of identical 'deformable' spheres into two or more size- or shape-distinct sets of particles. Significant challenges that must still be addressed to advance the field of soft matter FK phases further, however, include their rare and unpredictable occurrence, uncertain mechanisms of solid-state assembly, and low thermodynamic stability. Here we show that a readily-accessible sugar-polyolefin conjugate quantitatively produces an exceptionally stable solid-state FK A15 phase through a rapid and irreversible thermotropic order-order transition, which contrary to other prevailing proposed mechanisms, does not require mass transfer between particles or large structural reorganization in the bulk to establish unit cell non-equivalency. Our results provide the basis for a realistic strategy for obtaining practical and scalable quantities of a diverse range of sugar-polyolefin FK A15 phases with unique intrinsic physical properties and chemical reactivities not previously seen for soft matter FK phases.